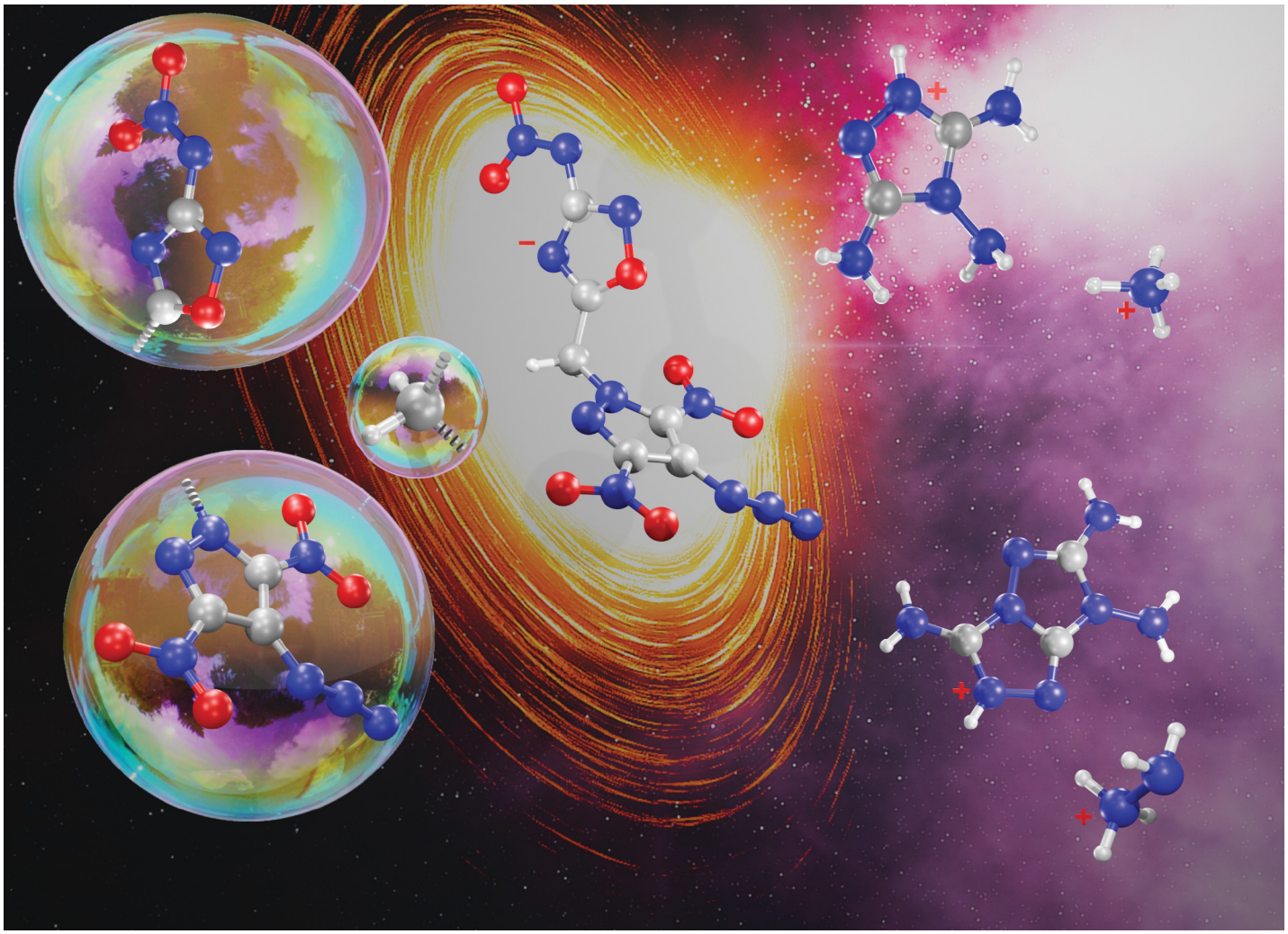

Showcasing research from Professor Dheeraj Kumar's laboratory, Department of Chemistry, Indian Institute of Technology Roorkee, Roorkee, India.

Taming of 4-azido-3,5-dinitropyrazole based energetic materials

4-Azido-3,5-dinitropyrazole (AzDNP) and its derivatives are attractive candidates as green energetic materials due to their excellent energetic properties and high nitrogen and oxygen contents. However, they are often more sensitive (primary explosives) and have poor thermal stability (T_d < 150 °C), attributed to the presence of azido functionality. In this work, we have tried to fine-tune the properties of 4-azido-3,5-dinitropyrazole by connecting it to 5-nitramino-1,2,4-oxadiazole moieties *via* *N*-methylene-*C* bridges and by energetic salts formation. The structure-property relationship was studied using Hirshfeld surface and Non-Covalent Interaction (NCI) analysis.

As featured in:

See Dheeraj Kumar *et al.*, *Mater. Adv.*, 2024, **5**, 171.

ROYAL SOCIETY OF CHEMISTRY

rsc.li/materials-advances

Registered charity number: 207890

Materials Advances

ROYAL SOCIETY OF CHEMISTRY

PAPER

View Article Online
View Journal | View Issue

Cite this: *Mater. Adv.*, 2024, 5, 171

Taming of 4-azido-3,5-dinitropyrazole based energetic materials†

Priyanka Das, Prachi Bhatia, Krishna Pandey and Dheeraj Kumar *

4-Azido-3,5-dinitropyrazole (AzDNP) and its derivatives are attractive candidates as high-performance energetic materials due to their excellent energetic properties and high nitrogen and oxygen contents. However, they are often more sensitive (primary explosives) and have poor thermal stability (T_d < 150 °C), attributed to the presence of the azido functionality. In this work, we have tried to fine-tune the properties of 4-azido-3,5-dinitropyrazole by connecting it to 5-nitramino-1,2,4-oxadiazole moieties *via* *N*-methylene-*C* bridges. Furthermore, a series of nitrogen-rich energetic salts (compounds **7–17**) were prepared from neutral compound **6** by reacting with different nitrogen-rich bases. All compounds were thoroughly characterized using IR and multinuclear NMR spectroscopy, differential scanning calorimetry (DSC), elemental analysis, and HRMS studies. Compounds **4**, **7**, and **9** were further confirmed through single-crystal X-ray diffraction studies. The physicochemical and energetic properties of all energetic compounds were also investigated. A hydroxylammonium salt, **12** (D_v: 8961 m s^{-1}; *P*: 33.0 GPa), has been found to be the most energetic derivative of AzDNP to date. Compounds **6** (D_v: 8734 m s^{-1}; *P*: 33.9 GPa; IS < 2.5 J) and **12** (D_v: 8961 m s^{-1}; *P*: 33.0 GPa; IS < 2.5 J) show potential to be used as metal-free high-performance primary explosives. The most comprehensive properties are shown by ammonium salt **7** (D_v: 8591 m s^{-1}; *P*: 30.6 GPa, T_d: 173 °C; IS: 14 J). The structure–property relationship was studied using Hirshfeld surface and non covalent interaction (NCI) analyses.

Received 20th September 2023,
Accepted 1st November 2023

DOI: 10.1039/d3ma00742a

rsc.li/materials-advances

Introduction

Since the discovery of the first known explosive, gunpowder, the high energy density material (HEDM) field has significantly helped humankind in defense, space exploration and civilian applications.[1–4] Low explosives include propellants and pyrotechnics, which undergo deflagration, whereas high explosives undergo detonation. High explosives are further classified as primary and secondary explosives based on their susceptibility to initiation. Due to their fast deflagration-to-detonation transition (DDT), primary explosives are used as initiators for less sensitive and high-performance secondary explosives.[5] The most commonly used primary explosives are based on toxic heavy metals like lead (*e.g.*, lead azide and lead styphnate) and mercury (*e.g.*, mercury fulminate) and cause severe threats to human health and the environment.[6] Similarly, the conventional secondary explosive, RDX (1,3,5-trinitro-1,3,5-triazinane), is a human carcinogen and toxic to important organisms at the bottom of the food chain.[7] Due to these concerns associated with traditional explosives, modern energetic materials should be environmentally friendly and should exhibit high performance and stability.[8–10] These problems can be solved using greener synthetic approaches, by fine-tuning at the molecular level and generating greener decomposition products (inert N_2 gas).

The modern energetic materials are based on five- and six-membered nitrogen-rich aromatic heterocyclic rings *e.g.*, azoles, oxadiazoles, triazines, tetrazines, *etc.*[11–20] These nitrogen-rich rings have high positive heats of formation and produce large amounts of nontoxic dinitrogen (N_2) gas upon detonation.[21] The presence of nitrogen-rich explosophores like azido ($-N_3$) in the energetic materials can further improve their heats of formation and increase the overall nitrogen content making them greener.[22–24] Among the five-membered nitrogen-rich heterocycles, 4-substituted-3,5-dinitropyrazole-based energetic compounds are the most explored, and their properties can be controlled depending on the substituent at the 4th position.[25] Substituents capable of forming intramolecular hydrogen bonds (*e.g.*, $-NH_2$ and –OH) tend to improve the stability of the resulting compounds, whereas electron withdrawing substituents (*e.g.*, $-NHNO_2$ and $-NO_2$) make them sensitive. 4-Azido-3,5-dinitropyrazole (AzDNP) with 49.35% nitrogen content and a high positive heat of formation (ΔH_f = 473 kJ mol^{-1}) is a good contender for high-performance energetic materials. AzDNP and its energetic salts have been

Energetic Materials Laboratory, Department of Chemistry, Indian Institute of Technology Roorkee, Roorkee-247667, Uttarakhand, India.
E-mail: dheeraj.kumar@cy.iitr.ac.in

† Electronic supplementary information (ESI) available. CCDC 2287540–2287542. For ESI and crystallographic data in CIF or other electronic format see DOI: https://doi.org/10.1039/d3ma00742a

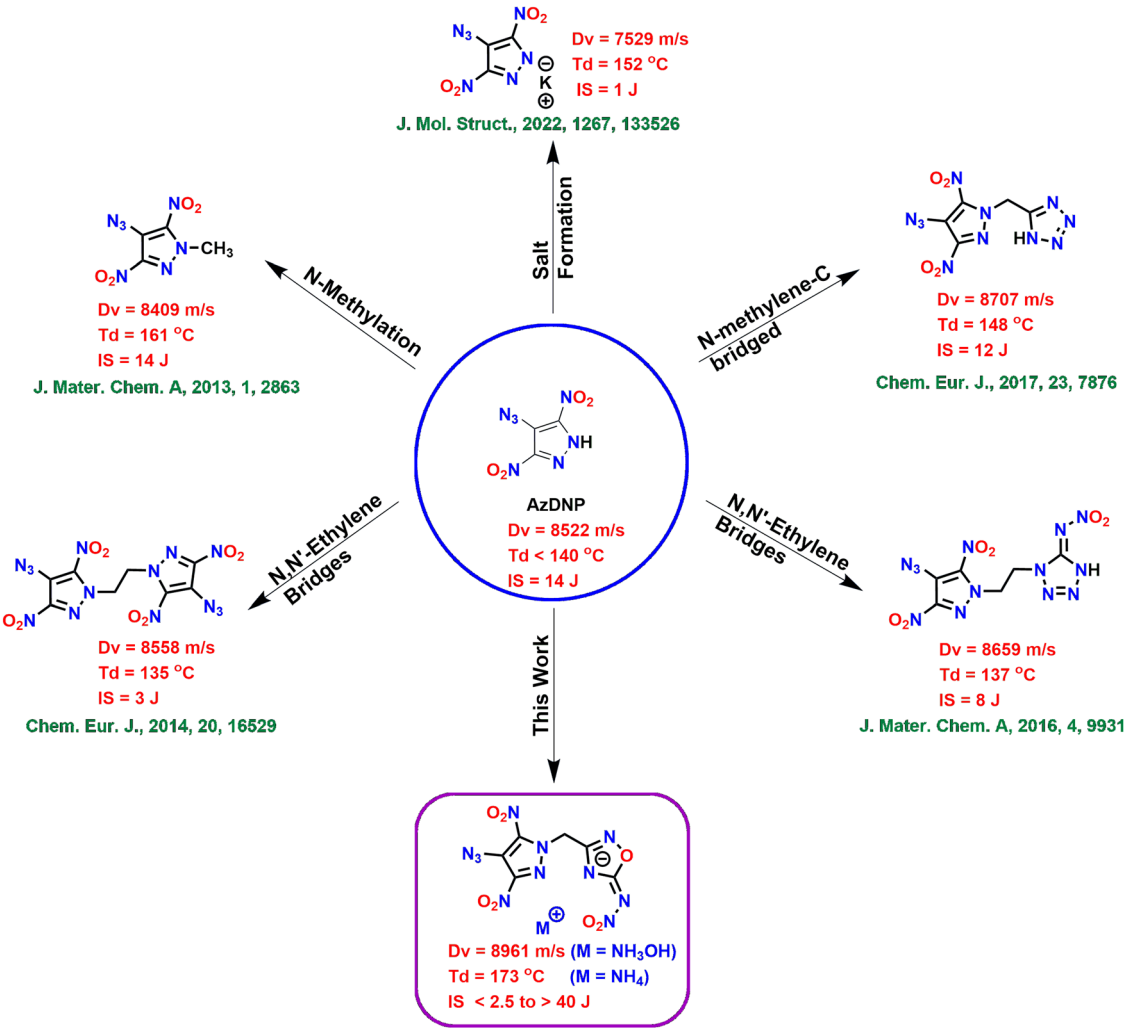

Fig. 1 Various approaches to improve the stability of AzDNP.

synthesized recently starting from 4-amino-3,5-dinitropyrazole (LLM-116), and they were found to be highly sensitive and found to exhibit poor thermal stability.[26] Shreeve and coworkers have used several approaches to improve the energetic and stability performance of AzDNP-based energetic compounds, such as (i) *N*-methylation,[25] (ii) *N*-methylene-*C* bridging with the tetrazole ring,[27] (iii) symmetric *N*,*N*′-ethylene bridging,[28] and (iv) asymmetric *N*,*N*′-ethylene bridging with nitroiminotetrazole;[29–31] however, most of these approaches result in compounds with either reduced energetic performance or poor thermal/physical stability (Fig. 1). Therefore, there is still scope for improvement in the overall performance of AzDNP-based energetic materials by combining them with more suitable energetic scaffolds.

Among all the isomers of oxadiazole, 1,2,4-oxadiazole is the most thermally stable framework and can also help improve the oxygen balance of the resulting energetic material.[32] Consequently, 5-amino-1,2,4-oxadiazole-based compounds have gained attention as scaffolds for many advanced energetic materials. A further enhancement of their energetic properties can be achieved by converting the amino group at 5th position to the nitroimino group.[33–35] Therefore, in this work, we have synthesized high-performance energetic materials consisting of the 4-azido-3,5-dinitropyrazole moiety linked with 5-nitramino-1,2,4-oxadiazole through *N*-methylene-*C* bridges. Since we aim to improve the stability (thermal/physical) of AzDNP-based energetic compounds without compromising their energetic properties, various nitrogen-rich energetic salts were also synthesized by reacting the acidic NH of the nitroimino moiety with different nitrogen-rich bases. This study shows that this approach has resulted in superior energetic derivatives of AzDNP. The parent neutral compound **6** is found to have better detonation properties and a higher density value than all other alkyl bridged AzDNP based energetic materials. Also, in many cases, salt formation has further improved the thermal and physical stability of the resulting energetic materials, making them suitable for practical application.

Results and discussion

Synthesis

The starting material, the *N*-acetonitrile derivative of 4-chloro-3,5-dinitropyrazole, **1** was synthesized using a procedure

described in the literature.[27] Reaction of **1** with hydroxylamine hydrochloride in the presence of a base ($NaHCO_3$) resulted in hydroxyacetimidamide derivative **2** as an orange-colored solid in 79% yield. Compound **3** with *N*-methylene-*C* linked 4-chloro-3,5-dinitropyrazole and 4-amino-1,2,4-oxadiazole was obtained in 73% yield by the cyclization of the hydroxyacetimidamide moiety in **2** using cyanogen bromide and $KHCO_3$. Compound **4** was obtained in 83% yield *via* the nucleophilic substitution of chloro in **3** with azido (N_3) by reaction with sodium azide in DMSO. Nitration of **3** with 100% nitric acid resulted in **5** (70% yield) with 4-chloro-3,5-dinitropyrazole and 4-nitroimino-1,2,4-oxadiazole rings connected through an *N*-methylene-*C* bridge. Compound **6** (could not be synthesized by the nitration of **4**) was obtained by the reaction of **5** with sodium azide followed by acidification as a white solid in 88% yield. Furthermore, to fine-tune their properties, energetic salts **7–17** were prepared. Energetic salts **7–10** were obtained directly by the reaction of **6** with various nitrogen-rich bases in acetonitrile, whereas energetic salts **12–17** were obtained by a metathesis reaction of a silver salt (compound **11**) with respective hydrochloride bases in water (Scheme 1).

Spectral studies of compounds

All newly synthesized compounds were fully characterized using FTIR and NMR [^{1}H, ^{13}C{^{1}H} and, in some cases, ^{15}N] spectroscopy and elemental analysis. In the ^{1}H and ^{13}C{^{1}H} NMR spectra of compounds **2–17**, signals due to the methylene bridge were seen in the ranges of 5.81–5.94 ppm and 50.58–51.13 ppm, respectively. Also, it was observed that in the ^{13}C{^{1}H} NMR spectra of energetic salts **7–17**, signals corresponding to methylene carbon were slightly deshielded (51.01–51.13 ppm) compared to the neutral compound **6** (50.87 ppm). The signals corresponding to the amino substituted carbon of the 1,2,4-oxadiazole ring in **3** and **4** were found to be upfield shifted at 172.28 ppm compared to those of the nitroimino substituted carbon of the 1,2,4-oxadiazole ring in **5** (174.25 ppm) and **6** (174.39 ppm). The corresponding signals of nitroimino substituted carbon in energetic salts **7–17** were observed at 175.13–175.36 ppm.

In addition to the ^{1}H and ^{13}C{^{1}H} NMR spectra, the ^{15}N NMR spectra were recorded for **4**, **6** and **17** in DMSO-d_6. The chemical shifts were assigned by taking liquid ammonia as a reference. The peaks are assigned based on comparison with similar reported compounds (Fig. 2).[27,36,37] The signals corresponding to the pyrazole ring nitrogen attached to the methylene bridge (N1) were observed between −192.21 and −193.18 ppm, whereas those for the other ring nitrogen (N2) were found to be downfield shifted between −80.69 and −80.94 ppm. The signals for oxadiazole ring nitrogens were observed in the ranges of −48.20 to −50.18 ppm (for N6) and −179.37 to −210.99 ppm (for N7). The signals (N3 and N4) for the nitro groups attached to the pyrazole rings showed resonance between −30.29 and −35.91 ppm, whereas the signal (N9) for the nitro group attached to the nitroimino moiety of the oxadiazole ring was slightly downfield shifted at −20.46 (compound **6**) and −17.65 ppm (compound **17**). For neutral compounds **4** and **6**, the characteristic signals due to the azido ($-N_3$) functionality were observed at [−151.48 (N5β), −152.44 (N5γ), −306.12 (N5α)] and [−151.42 (N5β), −152.57 (N5γ), −306.16 (N5α)] ppm, respectively. For salt **17**, azide signals were found

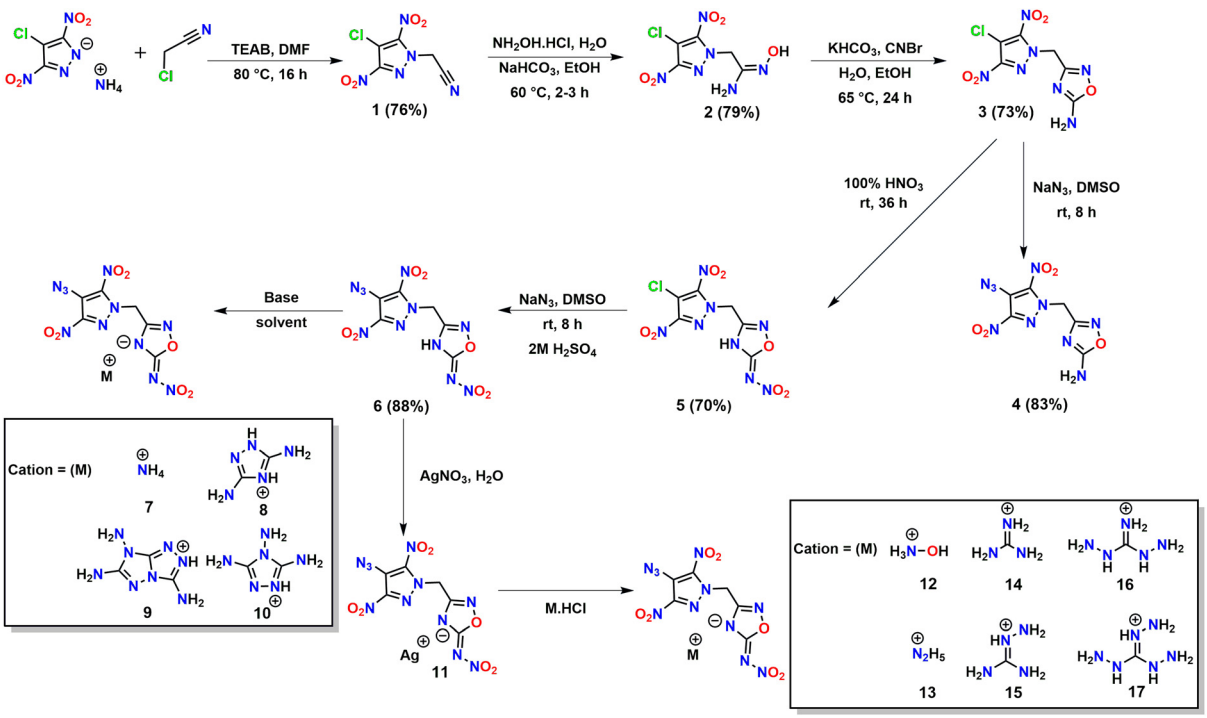

Scheme 1 Synthesis of energetic compounds **2–17**.

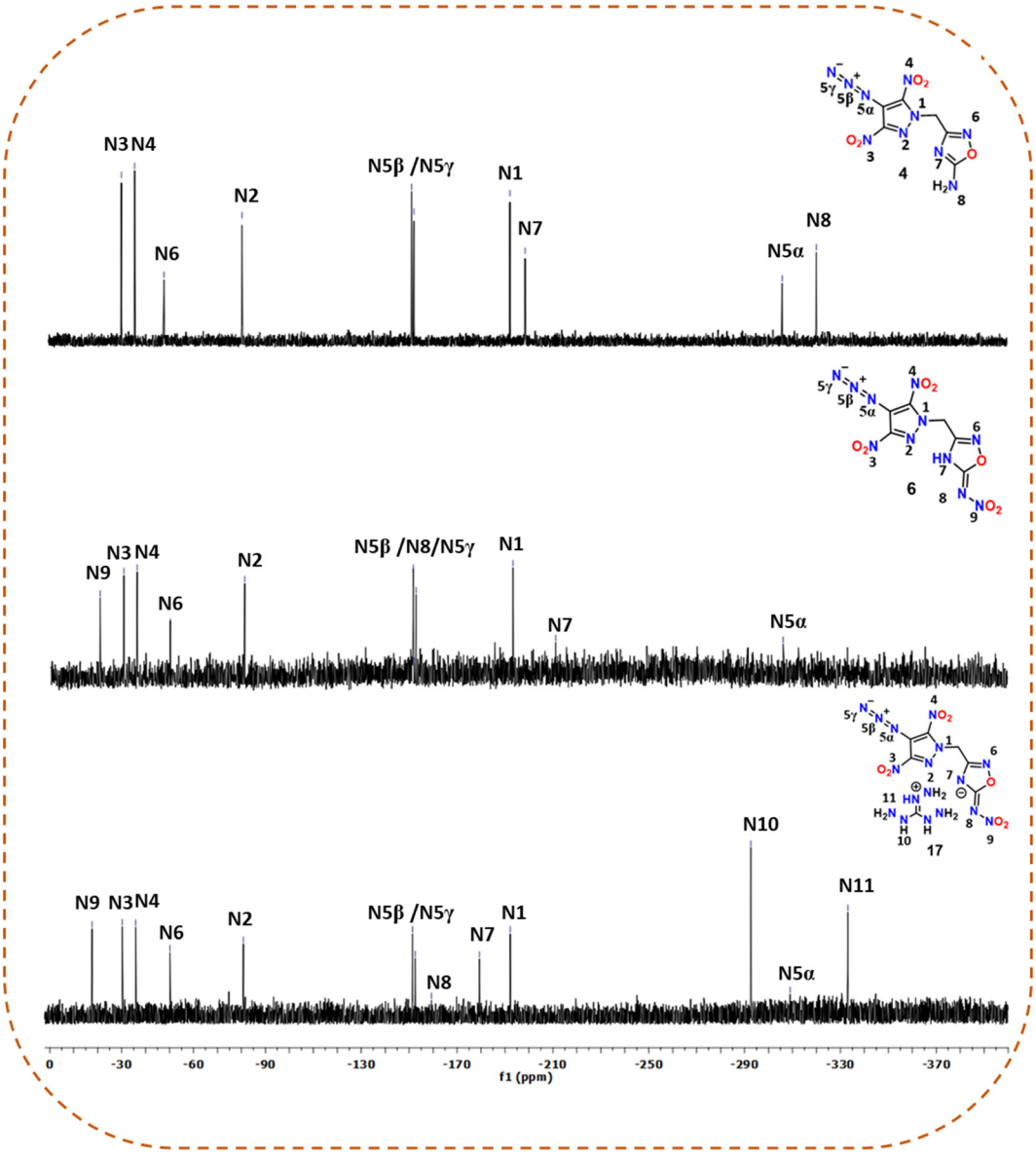

Fig. 2 ^{15}N NMR spectra of compounds **4**, **6**, and **17**.

to be slightly upfield shifted at −151.42 (N5β), −152.59 (N5α), and −308.98 (N5α) ppm. The signal corresponding to the NH_2 group in **4** was found to be the most shielded at −320.38 ppm. The triaminoguanidinium cation in **17** showed two distinct signals at −292.64 and −333.08 ppm.

Crystal structures

The structures of **4**, **7**, and **9** were confirmed by single-crystal X-ray analysis. Suitable single crystals were obtained by slow evaporation of their saturated solutions in acetonitrile/water or methanol/water mixtures. Detailed crystallographic information, data collection parameters, selected bond lengths, and bond angles are provided in the ESI.† Compound **4** crystallizes in an orthorhombic space group $Pca2_1$ with a room temperature crystal density of 1.78 g cm^{-3}. The bridging methylene carbon shows a slight distortion from the tetrahedral geometry with an angle N(6)–C(4)–C(5) = 109.1(3)°. The dihedral angle between the mean planes through the pyrazole and oxadiazole rings was found to be 72.9(1)°. The C–N bond length of the *N*-methylene-*C* bridge in **4** is slightly shorter [C(4)–N(6) = 1.48(5) Å] compared to the C–C bond length [C(4)–C(5) = 1.51(6) Å]. The two nitro groups on pyrazole ring were found to be slightly out of the plane of the pyrazole ring with the dihedral angles of 10.3(3)° and 14.7(2)°. The C–N bond length of the C–N_3 group was found to be slightly shorter [C(2)–N(3) = 1.38 (5) Å] compared to the C–N bond lengths of C–NO_2 groups [C(3)–N(2) = 1.42(5) and C(1)–N(1) = 1.45(5) Å]. The azide functional group is twisted with respect to the pyrazole ring, with the angle between the mean plane through the pyrazole ring and azido groups being 12.6(5)°. The crystal packing of **4** showed strong intermolecular

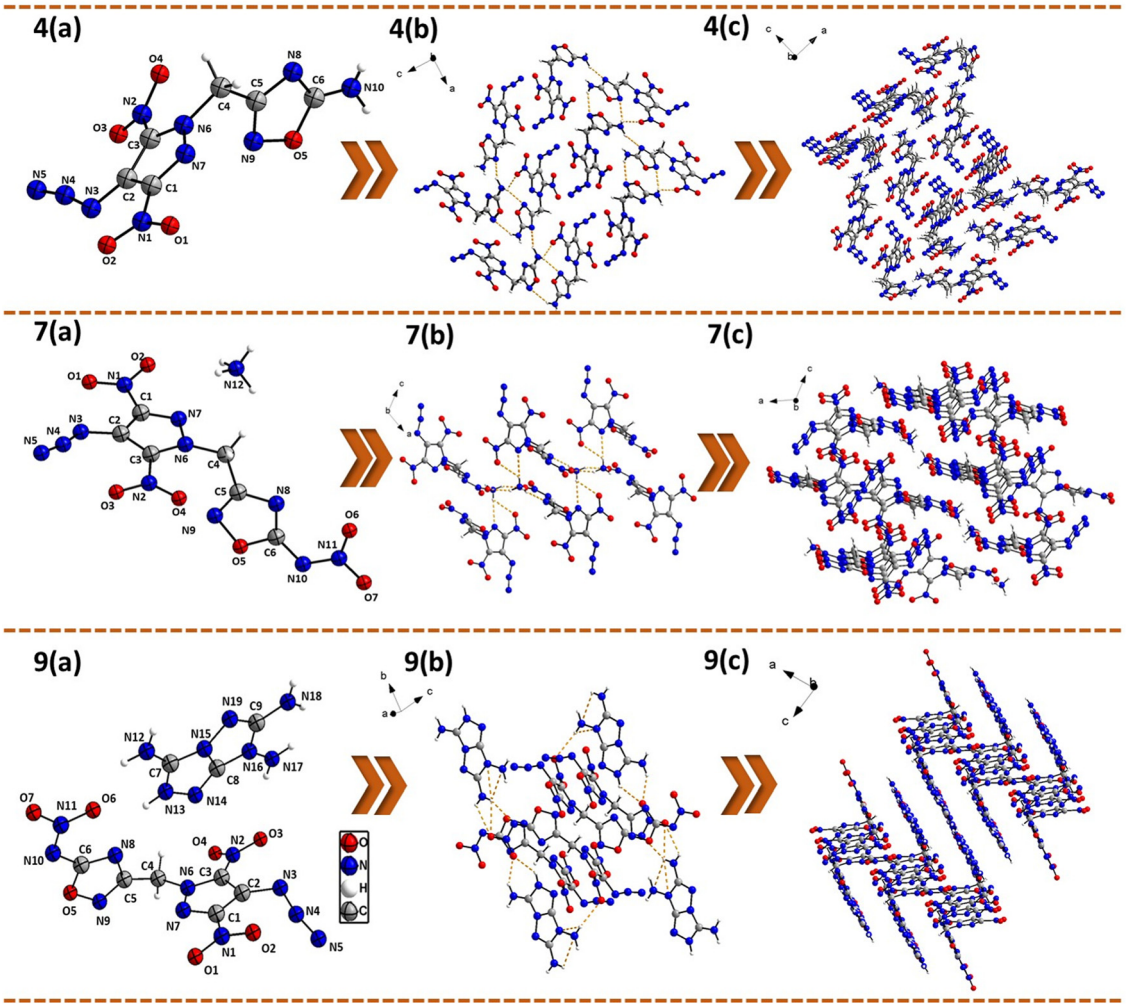

Fig. 3 (a) Thermal ellipsoid plot (50%) and the labeling scheme of compounds (**4**, **7**, and **9**). (b) Amplification of hydrogen bonding distribution in the labeled part of compounds (**4**, **7**, and **9**). (c) Ball and stick crystal packing diagram of (**4**, **7**, and **9**) viewed along the *b* axis. Orange dotted lines represent intra- and intermolecular hydrogen bonds.

hydrogen bonding interactions [between the NH_2 group of one oxadiazole ring and the N(8) ring nitrogen of another molecule of the oxadiazole ring] and electrostatic interactions between the nitro and azido groups (Fig. 3).

Energetic salt **7** crystallizes in a monoclinic space group $P2_1/n$ with a crystal density of 1.81 g cm^{-3}, whereas **9** crystallizes in a triclinic space group $P\bar{1}$ with a crystal density of 1.75 g cm^{-3} at 298 K. Unlike **4**, the bridging methylene groups in **7** and **9** showed a larger distortion from the tetrahedral geometry (109.5°) with N(6)–C(4)–C(5) angles of 113.1(1) and 112.0(3)°, respectively. The C–C [C(4)–C(5) = 1.49(2) and 1.48(5) Å] and C–N [C(4)–N(6) = 1.46(2) and 1.47(4) Å] bond lengths of the *N*-methylene-*C* bridges in energetic salts **7** and **9** are shorter compared to those of neutral compound **4** [C(4)–C(5) = 1.51(6) Å and C(4)–N(6) = 1.48(5) Å]. The dihedral angles between the mean planes through the pyrazole and oxadiazole rings for compounds **7** and **9** were found to be 80.4(7)° and 72.9(1)°, respectively. In compound **9**, the oxadiazole ring and TATOT cation were found to be almost coplanar with a dihedral angle of 8.3(9)°. The N–O bond lengths of nitroimino–oxadiazole rings in **7** [N(9)–O(5) = 1.421(2) Å] and **9** [N(9)–O(5) = 1.405(4) Å] were found to be shorter compared to the N–O bond length of the amino-oxadiazole ring in **4** [N(9)–O(5) = 1.434(2) Å]. The nitro groups substituted on the pyrazole ring in **7** and **9** are nearly coplanar with dihedral angles in the range of 7.5(1)° to 11.5 (2)°. In contrast, the azido groups are significantly out of the plane of pyrazole rings with dihedral angles of 14.3(6) and 37.1(1)°, respectively. In compound **7**, the C–N_3 bond length [C(2)–N(3) = 1.38(3) Å] is shorter compared to C–NO_2 bond lengths [1.42(3)–1.44(2) Å], whereas in compound **9**, the C–N_3 and C–NO_2 bond lengths are almost the same [1.43(6)–1.44(5) Å]. The N(3)–N(4)–N(5) angles of the azide moiety are 166.3(2)° for **7** and 168.5(6)° for **9**, making these azide bonds almost linear. The crystal packing of **7** and **9** displays a network of extensive inter- and intramolecular hydrogen bonding interactions as shown in Fig. 3. In compound **7**, the ammonium cation showed hydrogen bonding with the oxygen atoms of the nitroimino group

[N(12)···O(6) = 2.91(2) and N(12)···O(7) = 2.86(2) Å], the ring nitrogen of the oxadiazole ring [N(12)···N(8) = 2.88(2) Å], and the pyrazole nitro group [N(12)···O(1) = 3.05(2) Å]. In compound **9**, the oxadiazole ring and TATOT cation were found to be almost coplanar with a dihedral angle of 8.3(9)°. Consequently, there are strong hydrogen bonding interactions between the oxadiazole nitro group and TATOT amino groups [N(12)···O(6) = 2.71(4) Å, N(13)···O(6) = 2.99(4) Å, N(18)···O(7) = 2.78(4) Å] and the oxadiazole ring nitrogen and TATOT amino group [N(8)···N(13) = 2.93(4) Å]. Additionally, the pyrazole attached nitro group also showed hydrogen bonding interactions with TATOT [N(17)···O(3) = 3.03(4) Å and N(13)···O(4) = 3.04(5) Å], resulting in a zigzag layered crystal packing. All these H-bonding and other weak interactions contribute significantly to the better thermal stability and reduced sensitivity of these energetic salts compared to compound **4**.

Hirshfeld surface analysis and NCI analysis

The Hirshfeld surface analysis of **4**, **7**, and **9** has been performed using the Crystal Explorer 17.5 software to gain deeper knowledge about the structure–property relationship.[38] The Hirshfeld surface, 2D fingerprint spectra, and percentage of close contact populations of **4**, **7**, and **9** are shown in Fig. 4. The red and blue dots on the Hirshfeld surfaces represent the high and low close-contact populations, respectively. The red dots in **4**, **7**, and **9** are found mainly on the edge of the plane, owing to the hydrogen bonding interactions (O···H and N···H interactions), which are represented by sharp spikes in the 2D fingerprint plot. The total hydrogen bonding interactions (O···H and N···H) in **4**, **7**, and **9** were found to be 38%, 40.2%, and 40.8%, respectively. The higher percentage of hydrogen bonding interactions in **7** and **9** makes them more thermally and physically stable as compared to neutral compound **4**.

The non-covalent interaction (NCI) analysis of compounds **4**, **7**, and **9** was performed using the Multiwifn software, and plots were analyzed using the VMD software (Fig. 5).[39–41] In NCI analysis, a large green-coloured isosurface indicates face-to-face π–π interactions, whereas the blue and green ellipses are mainly due to intramolecular hydrogen bonding. Due to cationic–anionic interactions, **7** and **9** showed larger green isosurface areas, as well as hydrogen bonding interactions, compared to compound **4**. Therefore, the existence of a large number of hydrogen bonding and strong π–π interactions leads to the enhanced physical stability (thermal stability and insensitivity) of **7** and **9** compared to **4**.

Physicochemical and energetic properties

The physicochemical and energetic properties of all energetic compounds were investigated and the results are summarized in Table 1. The densities were measured using a helium gas pycnometer at 298 K, and the values range between 1.69 (**14**) and 1.86 (**6**) g cm^{-3}. All compounds were found to be denser

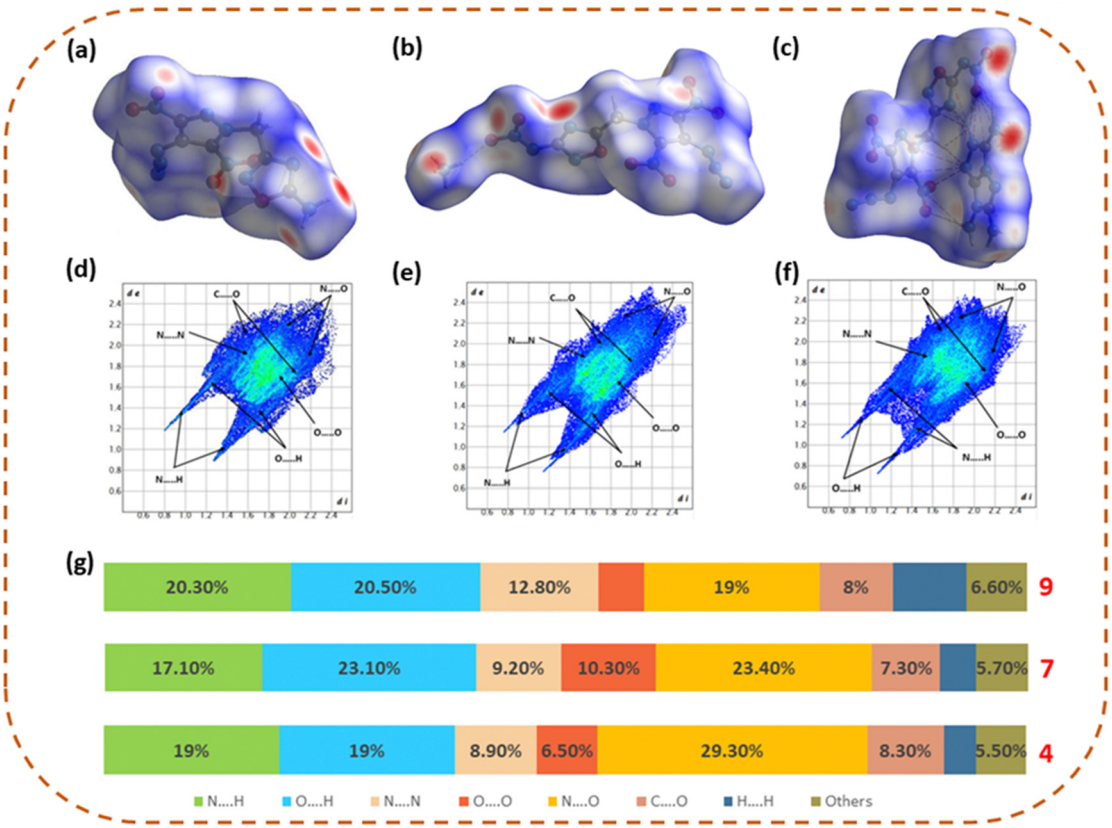

Fig. 4 Hirshfeld surfaces and fingerprint plots of **4** (a) and (d), **7** (b) and (e), and **9** (c) and (f) and the population of close contacts (g).

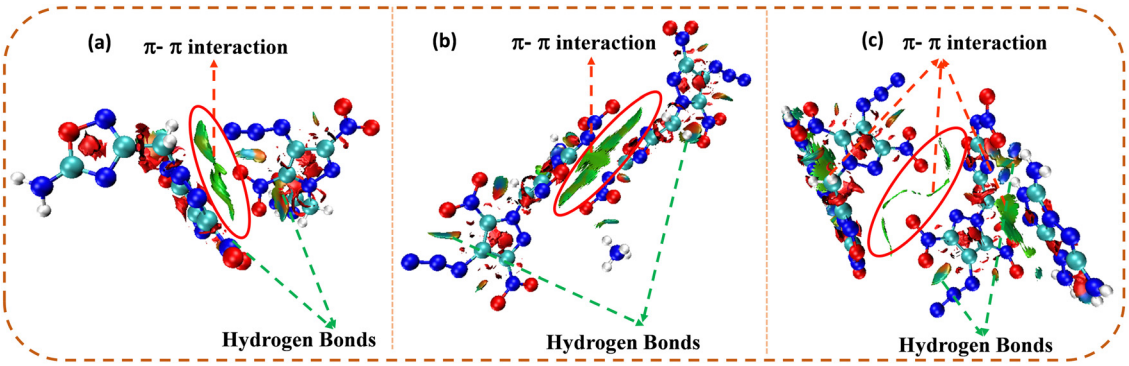

Fig. 5 NCI plots of compounds **4** (a), **7** (b), and **9** (c).

than TNT (1.65 g cm^{-3}), and neutral compound **6** (1.86 g cm^{-3}) exhibited a higher density than the traditional explosive RDX (1.80 g cm^{-3}). A significant decrease in the density values (from 1.80 to 1.69 g cm^{-3}) was observed for the energetic salts **7–17** compared to neutral compound **6**. The heats of formation (ΔH_f) were calculated using the Gaussian 09 program suite according to the isodesmic reaction (ESI†). All compounds showed high positive heats of formation, falling between 478.3 and 1049.4 kJ mol^{-1}, which surpass those of RDX (92.6 kJ mol^{-1}), TNT (−59.4 kJ mol^{-1}), and LA (450.1 kJ mol^{-1}). Among them, the 3,6,7-triamino-7*H*-[1,2,4]triazolo[4,3-*b*][1,2,4]triazol-2-ium (TATOT) salt, **9**, (1049.4 kJ mol^{-1}) exhibits the highest heat of formation value.

Based on the measured pycnometer densities and heat of formation values, the detonation properties (detonation velocity and detonation pressure) were computed using the EXPLO5 software (version 6.06).[23] The evaluated detonation velocities (D_v) range between 7923 and 8961 m s^{-1} and detonation pressures (P) between 24.3 and 33.9 GPa. All compounds exhibited a better detonation performance than the traditional explosive TNT (P: 21.3 GPa, D_v: 7303 m s^{-1}) and lead-based primary explosive LA (P: 33.4 GPa, D_v: 5877 m s^{-1}). Compounds **6** (P: 33.9 GPa, D_v: 8734 m s^{-1}), **7** (P: 30.6 GPa, D_v: 8591 m s^{-1}), **13** (P: 30.8 GPa, D_v: 8622 m s^{-1}) and **17** (P: 27.2 GPa, D_v: 8370 m s^{-1}) have energetic properties comparable to RDX (P: 34.9 GPa, D_v: 8795 m s^{-1}). Compound **12** (P: 33.0 GPa, Dv: 8961 m s^{-1}) displayed the highest detonation performance and was also found to be more energetic than RDX. Due to the large number of N–N, C–N, and O–N bonds, all these compounds were found to have excellent nitrogen contents (45–54%) that exceed those of RDX (38%), TNT (19%), and LA (28%). They also have good combined nitrogen + oxygen contents (74–79%), which also surpass that of TNT (61%) and are comparable to RDX (81%), indicating the environmentally friendly nature of these explosives.

Stability is another crucial factor for determining the overall performance of energetic compounds, which depends on thermal stability and mechanical sensitivity toward external stimuli. The decomposition temperature of compounds **4–17** was determined using differential scanning calorimetry (DSC) at a heating rate of 10 °C min^{-1} in a nitrogen atmosphere. The neutral amino-oxadiazole compound **4** decomposes at 146 °C, whereas nitroimino–oxadiazole **6** exhibits a sharp exothermic peak, with an onset decomposition temperature of 151 °C. Energetic salts **7–12**, **14**, and **15** showed a good improvement in the decomposition temperature compared to neutral

Table 1 Physicochemical and energetic properties of compounds **4–10** and **12–17**

Compound	ρ^a (g cm^{-3})	$D_v{}^b$ (m s^{-1})	P^c (GPa)	$T_m{}^d$ (°C)	$T_{dec}{}^e$ (°C)	$\Delta H_f{}^f$ (kJ mol^{-1})	IS^g (J)	FS^h (N)	N^i (%)	N + O^j (%)
4	1.78	8050	26.0	137	146	478.3	<2.5	60	47.29	74.30
6	1.86	8734	33.9	—	151	532.6	3.5	60	45.16	77.99
7	1.80	8591	30.6	—	173	550.2	14	240	46.93	78.20
8	1.71	7940	24.4	—	168	712.5	12	120	50.90	76.34
9	1.75	8184	26.1	—	164	1049.4	15	240	53.73	76.34
10	1.75	8224	26.6	156	160	827.1	>40	240	52.30	78.90
12	1.79	8961	33.0	—	152	595.6	<2.5	80	44.92	79.13
13	1.78	8622	30.8	—	146	696.5	15	120	48.79	78.80
14	1.69	7923	24.3	—	160	520.6	18	240	49.00	76.98
15	1.74	8230	26.6	—	152	607.9	>40	240	50.60	77.57
16	1.71	8219	26.3	—	136	715.1	<2.5	80	52.09	78.12
17	1.72	8370	27.2	—	132	820.6	5	120	53.48	78.63
RDX	1.80	8795	34.9	—	204	92.6	7.4	120	37.84	81.06
TNT	1.65	7303	21.3	—	295	−59.4	15	358	18.50	60.76
LA	4.80	5877	33.4	—	315	450.1	0.1–1	0.3–0.6	28.86	28.86

[a] Density measured using a gas pycnometer at 25 °C. [b] Calculated detonation velocity. [c] Calculated detonation pressure. [d] Melting point (onset). [e] Temperature of decomposition (onset). [f] Heat of formation. [g] Impact sensitivity. [h] Friction sensitivity. [i] Nitrogen content. [j] Combined nitrogen and oxygen contents.

compound **6**, with ammonium salt **7** (T_{dec} = 173 °C) exhibiting the highest thermal stability. At the same time, hydrazinium (**13**), diaminoguanidinium (**16**), and triaminoguanidinium (**17**) salts showed a lower thermal stability compared to neutral compound **6**. This is probably due to the additional number of acyclic N–N bonds present in these cations. Apart from **7** (T_{dec} = 173 °C), compounds **8** (T_{dec} = 168 °C), **9** (T_{dec} = 164 °C), **10** (T_{dec} = 160 °C), and **14** (T_{dec} = 160 °C) showed acceptable thermal stability with decomposition temperatures above 160 °C.

The sensitivities of all compounds towards impact (IS) and friction (FS) were evaluated using the BAM Fallhammer apparatus and BAM friction tester, respectively. Neutral compounds **4** and **6**, along with energetic salts **12** (hydroxylammonium) and **16** (diaminoguanidinium), are highly sensitive towards external stimuli with impact sensitivities of <4 J and friction sensitivities of <80 N, which categorized them as primary explosives. However, most of the other energetic salts were found to have improved sensitivity values compared to neutral compound **6** with impact sensitivity >10 J and friction sensitivity >120 N. Among all, **10** and **15** are found to be insensitive (IS: 40 J, FS: 240 N) towards impact and friction. All compounds are physically more stable than LA, whereas **7–10** and **13–15** exhibited lower sensitivities than the benchmark explosive RDX.

Conclusions

A new family of energetic materials based on 4-azido-3,5-dinitropyrazole and 5-nitramino-1,2,4-oxadiazole rings connected *via* *N*-methylene-*C* bridges were synthesized. This approach of connecting the 4-azido-3,5-dinitropyrazole moiety with another ring (5-nitramino-1,2,4-oxadiazole – capable of forming energetic salts) using a non-energetic methylene bridge resulted in some of the best energetic derivatives of AzDNP. This approach was found to be better compared to the direct salt formation, *N*-methylation, and *N*,*N*′-ethylene bridging strategies (Fig. 1). All energetic compounds were fully characterized, and their physicochemical and energetic properties were explored. The parent neutral compound **6** and its hydroxylammonium salt **12** are found to be the most energetic derivatives of AzDNP and showed energetic properties similar to RDX. Most energetic salts demonstrated improved thermal stability (up to 22 °C), impact sensitivity (5–35 J) and good energetic performance. We believe that this approach will pave the way for stabilizing azido-based energetic compounds with improved physical and thermal stabilities.

Experimental section

Caution!

Although no accidents were observed during the synthesis, handling, and characterization, all compounds reported in this work are potentially explosive materials and may explode unpredictably under certain conditions. All compounds must be synthesized only on a small scale (<100 mg). Any mechanical actions involving grinding or scratching must be avoided. In addition, all manipulations must be strictly carried out in a fume hood behind a polycarbonate safety shield. An eye protector, a face shield, and leather gloves must be worn while handling these compounds.

General methods

All reagents were purchased from Aldrich, TCI or GLR Innovations in analytical grade and were used as supplied, if not stated otherwise. ^{1}H, ^{13}C NMR and ^{15}N spectra were recorded using a 500 MHz (JEOL ECZ500R/S1) NMR spectrometer operating at 500, 125 and 50.69 MHz, respectively. As external standards, chemical shifts in the ^{1}H and ^{13}C NMR spectra are reported relative to Me_4Si and those in ^{15}N NMR to ammonia. The melting and decomposition temperatures were obtained using a differential scanning calorimeter (S11 6300 EXSTAR) at a scan rate of 10 °C min^{-1}. IR spectra were recorded using KBr pellets for solids on a PerkinElmer FT-IR spectrometer. HRMS spectra were recorded using the ESI-TOF technique. Densities were measured at room temperature by employing an Anton Paar Ultrapyc 5000 gas pycnometer. Quadrupole time-of-flight high resolution mass spectra (QTOF−HRMS) were obtained in the ESI mode. Elemental analyses were carried out on an Elementar model Vario-EI-III. The impact and friction sensitivity measurements were made using a standard BAM fall hammer (OZM) and a BAM Friction tester (FST ProEX).

Suitable crystals of **4**, **7**, and **9** were obtained by slow evaporation of their saturated solutions in acetonitrile/water and methanol/water mixtures, respectively. Single-crystal diffraction studies were carried out on a Bruker SMART APEX CCD diffractometer equipped with an Mo Kα (λ = 0.71073 Å) sealed tube. All crystal structures were solved by direct methods. The program SAINT (version 6.22) was used for the integration of the intensity of reflections and scaling. The program SADABS was used for absorption correction. The crystal structures were solved and refined using the SHELXTL (version 6.12) package.[42] All hydrogen atoms were included in idealized positions, and a riding model was used. Non-hydrogen atoms were refined with anisotropic displacement parameters.

Theoretical study

The heats of formation of energetic compounds **4–17** were obtained by using isodesmic reactions. The geometric optimization and frequency analyses of the structures were performed at the B3PW91/6-31G(d,p) level without any symmetry restrictions as implemented in the Gaussian 09 program.[43,44] All optimized derivatives are confirmed to be true local energy minima on the potential energy surface without any imaginary frequencies. All calculated gas-phase enthalpies for covalent materials are converted to solid-phase values by subtracting the empirical heat of sublimation obtained based on the molecular surface properties.[45] For salts **7–17**, the solid phase heats of formation were calculated based on the Born–Haber energy cycle.[46,47]

2-(4-Chloro-3,5-dinitro-1*H*-pyrazol-1-yl)-*N*′-hydroxyacetimidamide (2). To a stirred solution of hydroxylamine hydrochloride (1.35 g, 19.5 mmol) and sodium bicarbonate (1.64 g, 19.5 mmol)

in 75 mL of water was added a suspension of **1** (3.00 g, 13.0 mmol) in ethanol (10 mL) and the reaction mixture was stirred at 60 °C for 3 h. After cooling, orange-coloured crystals were obtained, which were filtered, washed with water (10 mL), and dried in air to yield **2**. Yield: 2.70 g, 79%. ^{1}H NMR (DMSO-d_6, ppm): 9.33 (s, 1H, O*H*), 5.79 (s, 2H, NH_2), 5.30 (s, 2H, CH_2). ^{13}C{^{1}H} NMR (DMSO-d_6, ppm): δ 148.2, 146.6, 143.0, 105.8, 54.3 ppm. IR (ν, cm^{-1}): 3604, 3469, 3369, 3195, 1684, 1567, 1509, 1330, 1067, 965, 882, 795, 686. Elemental analysis of $C_5H_5ClN_6O_5$ (264.58): calcd: C 22.70, H 1.90, N 31.76%. Found: C 22.16, H 1.81, N 30.97%.

3-((4-Chloro-3,5-dinitro-1*H*-pyrazol-1-yl)methyl)-1,2,4-oxadiazol-5-amine (3). To a solution of **2** (2.00 g, 7.6 mmol) in the ethanol (25 mL) and water (50 mL) mixture was added potassium bicarbonate (2.66 g, 26.6 mmol) and cyanogen bromide (2.81 g, 26.6 mmol), and the reaction mixture was stirred at room temperature for 24 h. The precipitate obtained was filtered, washed with water (15 mL), and dried in air to yield **3** as an off-white solid. Yield: 1.60 g, 73%. ^{1}H NMR (DMSO-d_6, ppm): 8.03 (s, 2H, NH_2), 5.86 (s, 2H, CH_2). ^{13}C{^{1}H} NMR (DMSO-d_6, ppm): δ 172.3, 164.7, 148.6, 142.5, 106.5, 50.8 ppm. IR (ν, cm^{-1}): 3378, 3164, 3023, 1667, 1563, 1505, 1438, 1328, 1282, 1064, 887, 788. Elemental analysis of $C_6H_4ClN_7O_5$ (289.59): calcd: C 24.89, H 1.39, N 33.86%. Found: C 24.79, H 1.33, N 33.76%.

3-((4-Azido-3,5-dinitro-1*H*-pyrazol-1-yl)methyl)-1,2,4-oxadiazol-5-amine (4). Sodium azide (0.34 g, 5.2 mmol) was added in one portion to a solution of **3** (0.50 g, 1.7 mmol) in DMSO (25 mL). The solution was stirred at room temperature for 8 h and then poured into ice water (20 mL). The resulting solution was stirred at room temperature for 30 min. The precipitate obtained was filtered, washed with cold water (5 mL), and dried in air to yield **5** as an orange solid. Yield: 0.42 g, 83%. ^{1}H NMR (DMSO-d_6, ppm): 8.02 (s, 2H, NH_2), 5.81 (s, 2H, CH_2). ^{13}C{^{1}H} NMR (DMSO-d_6, ppm): δ 172.3, 164.9, 145.1, 137.3, 117.5, 50.6 ppm. ^{15}N NMR (DMSO-d_6): −30.4, −35.9, −48.2, −80.7, −151.5, −152.4, −192.5, 198.9, −306.1, 320.4. IR (ν, cm^{-1}): 3350, 3144, 2144, 1669, 1581, 1512, 1443, 1324, 919, 801, 757. Elemental analysis of $C_6H_4N_{10}O_5$ (296.16): calcd: C 24.33, H 1.36, N 47.29%. Found: C 24.38, H 1.51, N 46.95%.

***N*-(3-((4-Chloro-3,5-dinitro-1*H*-pyrazol-1-yl)methyl)-1,2,4-oxadiazol-5(4*H*)-ylidene)nitramide (5).** Compound **3** (1.00 g, 3.5 mmol) was added carefully to ice-cold 100% HNO_3 (28 mL). The solution was then slowly warmed to room temperature and stirred for 36 h. Nitric acid was removed under compressed air, and the solid residue obtained was washed with a hexane/EtOAc (3 : 1) solution and dried in air to obtain **5** as a white solid. Yield: 0.80 g, 70%. ^{1}H NMR (DMSO-d_6, ppm): 8.24 (s, 1H, N*H*), 5.94 (s, 2H, CH_2). ^{13}C{^{1}H} NMR (DMSO-d_6, ppm): δ 174.2, 163.5, 148.7, 142.6, 106.6, 51.1 ppm. IR (ν, cm^{-1}): 3459, 3242, 3022, 1844, 1590, 1510, 1448, 1327, 1274, 1177, 1065, 962, 896, 793, 722. Elemental analysis of $C_6H_3ClN_8O_7$ (334.59): calcd: C 21.54, H 0.90, N 33.49%. Found: C 21.45, H 1.11, N 33.26%.

***N*-(3-((4-Azido-3,5-dinitro-1*H*-pyrazol-1-yl)methyl)-1,2,4-oxadiazol-5(4*H*)-ylidene)nitramide (6).** Sodium azide (0.30 g, 4.5 mmol) was added in one portion to a solution of **5** (0.50 g, 1.5 mmol) in DMSO (25 mL). The solution was stirred at room temperature for 8 h and poured into ice water (20 mL). The aqueous solution was acidified to pH 1–2 with 2 M sulfuric acid, and the resulting solution was stirred at room temperature for 30 min. The precipitate was filtered, washed with cold water (5 mL), and dried in air to obtain **6** as an off-white solid. Yield: 0.45 g, 88%. ^{1}H NMR (DMSO-d_6, ppm): 5.90 (s, 2H, CH_2). ^{13}C{^{1}H} NMR (DMSO-d_6, ppm): δ 174.4, 163.8, 145.2, 137.4, 117.5, 50.9 ppm. ^{15}N NMR (DMSO-d_6): −20.5, −30.4, −36.0, −49.8, −80.9, −151.4, −151.9, −152.6, −193.2, −211.0, −306.2. IR (ν, cm^{-1}): 3462, 3254, 3020, 2220, 2135, 1616, 1512, 1449, 1327, 1271, 1074, 970, 797, 724. Elemental analysis of $C_6H_3N_{11}O_7$ (341.16): calcd: C 21.12, H 0.89, N 45.16%. Found: C 21.16, H 1.01, N 44.82%. HRMS (ESI) *m*/*z* [M–H]$^-$ calcd for $C_6H_3N_{11}O_7$ 340.0139, found: 340.0166.

Ammonium 3-((4-azido-3,5-dinitro-1*H*-pyrazol-1-yl)methyl)-5-(nitroimino)-1,2,4-oxadiazol-4-ide (7). Compound **6** (0.20 g, 0.6 mmol) was dissolved in acetonitrile (3 mL), and a solution of 28% aqueous ammonia (20 mg, 0.6 mmol) in acetonitrile (1 mL) was added to it. The resulting solution was stirred at room temperature for 2 h. Afterward, the solvent was reduced in air pressure to yield **7** as a light-yellow solid. Yield: 0.17 g, 81%. ^{1}H NMR (DMSO-d_6, ppm): 7.09 (t, 4H, NH_4^+), 5.87 (s, 2H, CH_2). ^{13}C{^{1}H} NMR (DMSO-d_6, ppm): δ 175.2, 164.4, 145.1, 137.2, 117.4, 51.1 ppm. IR (ν, cm^{-1}): 3459, 3254, 2149, 1587, 1519, 1433, 1402, 1320, 1291, 1089, 919, 806, 730. Elemental analysis of $C_6H_6N_{12}O_7$ (358.19): calcd: C 20.12, H 1.69, N 46.93%. Found: C 20.19, H 1.81, N 46.86%.

3,5-Diamino-1*H*-1,2,4-triazol-4-ium(*Z*)-3-((4-azido-3,5-dinitro-1*H*-pyrazol-1-yl)methyl)-5-(nitroimino)-1,2,4-oxadiazol-4-ide (8). Compound **6** (0.20 g, 0.6 mmol) was suspended in water (5 mL), and a solution of 3,5-diamino-1*H*-1,2,4-triazol-4-ium (0.57 g, 0.6 mmol) in water (3 mL) was added. The resulting solution was stirred at room temperature for 4 h, and afterward, the solvent was reduced to about 2 mL by blowing air. The precipitate obtained was filtered, washed with water (1 mL), and dried in air to yield **8** as a light-yellow solid. Yield: 0.23 g, 89%. ^{1}H NMR (DMSO-d_6, ppm): 6.97 (s, 4H, NH_2), 5.87 (s, 2H, CH_2). ^{13}C{^{1}H} NMR (DMSO-d_6, ppm): δ 175.4, 164.3, 151.5, 145.1, 137.5, 117.6, 51.1 ppm. IR (ν, cm^{-1}): 3605, 3444, 3192, 2700, 2123, 1706, 1669, 1582, 1432, 1372, 1270, 1001, 901, 775, 735. Elemental analysis of $C_8H_8N_{16}O_7$ (440.26): calcd: C 21.83, H 1.83, N 50.90%. Found: C 21.77, H 1.93, N 50.77%.

3,6,7-Triamino-7*H*-[1,2,4]triazolo[4,3-*b*][1,2,4]triazol-2-ium(*Z*)-3-((4-azido-3,5-dinitro-1*H*-pyrazol-1-yl)methyl)-5-(nitroimino)-1,2,4-oxadiazol-4-ide (9). Compound **6** (0.20 g, 0.6 mmol) was dissolved in acetonitrile (5 mL), and a suspension of 3,6,7-triamino-7*H*-[1,2,4]triazolo[4,3-*b*][1,2,4]triazol-2-ium (0.90 g, 0.6 mmol) in acetonitrile (3 mL) was added. The resulting solution was stirred at room temperature for 2 h, and afterward, the solvent was reduced to about 2 mL by blowing air. The precipitate obtained was filtered, washed with acetonitrile (1 mL), and dried in air to yield **9** as a white solid. Yield: 0.25 g, 86%. ^{1}H NMR (DMSO-d_6, ppm): 8.13 (s, 2H, NH_2), 7.21 (s, 2H, NH_2), 5.86 (s, 2H, CH_2), 5.76 (s, 2H, NH_2). ^{13}C{^{1}H} NMR (DMSO-d_6, ppm): δ 175.3, 164.5, 160.2, 147.5, 145.1, 141.2, 137.4, 117.5, 51.1 ppm. IR (ν, cm^{-1}): 3379, 3104, 2162, 1685, 1659, 1584,

1519, 1312, 1091, 777, 713. Elemental analysis of $C_9H_9N_{19}O_7$ (495.30): calcd: C 21.83, H 1.83, N 53.73%. Found: C 21.77, H 1.85, N 52.58%.

3,4,5-Triamino-4*H*-1,2,4-triazol-1-ium(*Z*)-3-((4-azido-3,5-dinitro-1*H*-pyrazol-1-yl)methyl)-5-(nitroimino)-1,2,4-oxadiazol-4-ide (10). Compound **6** (0.20 g, 0.6 mmol) was suspended in water (5 mL), and a solution of 3,4,5-triamino-4*H*-1,2,4-triazol-1-ium (0.06 g, 0.6 mmol) in water (3 mL) was added. The resulting solution was stirred at room temperature for 4 h, and afterward, the solvent was reduced to about 2 mL by blowing air. The precipitate obtained was filtered, washed with water (1 mL), and dried in air to yield **10** as a golden-yellow solid. Yield: 0.22 g, 85%. ^{1}H NMR (DMSO-d_6, ppm): 7.09 (s, 4H, NH_2), 5.86 (s, 2H, CH_2), 5.58 (s, 2H, NH_2). ^{13}C{^{1}H} NMR (DMSO-d_6, ppm): δ 175.3, 164.3, 150.0, 145.1, 137.4, 117.5, 51.1 ppm. IR (ν, cm^{-1}): 3406, 3363, 2134, 1706, 1663, 1583, 1447, 1378, 1323, 1070, 899, 777. Elemental analysis of $C_8H_9N_{17}O_7$ (455.09): calcd: C 21.11, H 1.99, N 52.30%. Found: C 21.07, H 2.13, N 52.18%.

Silver (*Z*)-3-((4-azido-3,5-dinitro-1*H*-pyrazol-1-yl)methyl)-5-(nitroimino)-1,2,4-oxadiazol-4-ide (11). A solution of $AgNO_3$ (0.20 g, 1.2 mmol) in H_2O (16 mL) was added dropwise to a suspension of compound **6** (0.40 g, 1.2 mmol) in H_2O (10 mL) and stirred at room temperature for 2 h. The precipitate was collected, washed with water, and dried, giving **11** as a white solid. Yield: 0.42 g, 82%. ^{1}H NMR (DMSO-d_6, ppm): 5.92 (s, 2H, CH_2). ^{13}C{^{1}H} NMR (DMSO-d_6, ppm): δ 174.4, 163.8, 145.3, 137.5, 117.1, 51.0 ppm. IR (ν, cm^{-1}): 3453, 3269, 2140, 1784, 1587, 1522, 1448, 1331, 1084, 971, 908, 797, 728. Elemental analysis of $C_6H_2AgN_{11}O_7$ (448.02): calcd: C 16.09, H 0.45, N 34.39%. Found: C 16.17, H 0.63, N 34.17%.

General procedure for the synthesis of salts 12–17

A solution of hydroxylammonium chloride (0.06 g, 0.9 mmol), hydrazinium chloride (0.06 g, 0.9 mmol) guanidinium chloride (0.09 g, 0.9 mmol), aminoguanidinium chloride (0.10 g, 0.9 mmol), diaminoguanidinium chloride (0.11 g, 0.9 mmol), and triaminoguanidinium chloride (0.13 g, 0.9 mmol) in water (2 mL) was added dropwise to a suspension of precursor salt **11** (0.20 g, 0.45 mmol) in water (10 mL). The mixture was stirred at room temperature for 12 h under darkness. The precipitate was filtered off, and the filtrate was dried in air to obtain the product.

Hydroxylammonium (*Z*)-3-((4-azido-3,5-dinitro-1*H*-pyrazol-1-yl)methyl)-5-(nitroimino)-1,2,4-oxadiazol-4-ide (12). Yield: 0.14 g, 84%. Orange solid. ^{1}H NMR (DMSO-d_6, ppm): 10.29 (s, 4H, NH_3OH^+), 5.86 (s, 2H, CH_2). ^{13}C{^{1}H} NMR (DMSO-d_6, ppm): δ 175.1, 164.3, 145.2, 137.4, 117.5, 51.1 ppm. IR (ν, cm^{-1}): 3489, 2695, 2141, 1455, 1330, 1274, 1075, 1002, 903, 804, 778. Elemental analysis of $C_6H_6N_{12}O_8$ (374.19): calcd: C 19.26, H 1.62, N 44.92%. Found: C 19.07, H 1.73, N 44.88%.

Hydrazinium (*Z*)-3-((4-azido-3,5-dinitro-1*H*-pyrazol-1-yl)methyl)-5-(nitroimino)-1,2,4-oxadiazol-4-ide (13). Yield: 0.11 g, 66%. Yellow solid. ^{1}H NMR (DMSO-d_6, ppm): 6.35 (br, 5H, $N_2H_5^+$), 5.87 (s, 2H, CH_2). ^{13}C{^{1}H} NMR (DMSO-d_6, ppm): δ 175.2, 164.2, 145.1, 137.4, 117.4, 51.1 ppm. IR (ν, cm^{-1}): 3519, 2135, 1781, 1671, 1515, 1331, 1089, 953, 831, 801. Elemental analysis of $C_6H_7N_{13}O_7$ (373.21): calcd: C 19.31, H 1.89, N 48.79%. Found: C 19.27, H 1.83, N 48.66%.

Guanidinium (*Z*)-3-((4-azido-3,5-dinitro-1*H*-pyrazol-1-yl)methyl)-5-(nitroimino)-1,2,4-oxadiazol-4-ide (14). Yield: 0.14 g, 78%. Pale yellow solid. ^{1}H NMR (DMSO-d_6, ppm): 7.11 (s, 6H, NH_2), 5.86 (s, 2H, CH_2). ^{13}C{^{1}H} NMR (DMSO-d_6, ppm): δ 175.2, 164.3, 158.3, 145.1, 137.4, 117.4, 51.1 ppm. IR (ν, cm^{-1}): 3428, 3189, 2140, 1779, 1665, 1583, 1521, 1451, 1331, 1284, 1086, 996, 903, 804, 560. Elemental analysis of $C_7H_8N_{14}O_7$ (400.23): calcd: C 21.01, H 2.01, N 49.00%. Found: C 21.07, H 2.13, N 47.12%.

Aminoguanidinium (*Z*)-3-((4-azido-3,5-dinitro-1*H*-pyrazol-1-yl)methyl)-5-(nitroimino)-1,2,4-oxadiazol-4-ide (15). Yield: 0.15 g, 81%. Orange solid. ^{1}H NMR (DMSO-d_6, ppm): 8.78 (s, 1H, NH^+), 7.14 (br, 4H, NH_2), 5.86 (s, 2H, CH_2), 4.25 (s, 2H, NH_2). ^{13}C{^{1}H} NMR (DMSO-d_6, ppm): δ 175.2, 164.3, 159.1, 145.1, 137.4, 117.4, 51.0 ppm. IR (ν, cm^{-1}): 3368, 3167, 2347, 2214, 2138, 1767, 1675, 1635, 1517, 1431, 1329, 1277, 1204, 1074, 991, 903, 791. Elemental analysis of $C_7H_9N_{15}O_7$ (415.25): calcd: C 20.25, H 2.18, N 50.60%. Found: C 20.27, H 2.23, N 50.48%.

Diaminoguanidinium (*Z*)-3-((4-azido-3,5-dinitro-1*H*-pyrazol-1-yl)methyl)-5-(nitroimino)-1,2,4-oxadiazol-4-ide (16). Yield: 0.15 g, 78%. Orange solid. ^{1}H NMR (DMSO-d_6, ppm): 8.72 (s, 2H, NH), 7.24 (s, 2H, NH_2^+), 5.86 (s, 2H, CH_2), 4.02 (s, 4H, NH_2). ^{13}C{^{1}H} NMR (DMSO-d_6, ppm): δ 175.2, 164.3, 159.9, 145.0, 137.3, 117.4, 51.1 ppm. IR (ν, cm^{-1}): 3434, 3311, 3249, 2350, 2138, 1603, 1623, 1512, 1330, 1201, 997, 957. Elemental analysis of $C_7H_{10}N_{16}O_7$ (430.26): calcd C 19.54, H 2.34, N 52.09%. Found: C 19.57, H 2.43, N 51.88%.

Triaminoguanidinium (*Z*)-3-((4-azido-3,5-dinitro-1*H*-pyrazol-1-yl)methyl)-5-(nitroimino)-1,2,4-oxadiazol-4-ide (17). Yield: 0.16 g, 80%. Orange solid. ^{1}H NMR (DMSO-d_6, ppm): 8.59 (s, 3H, NH), 5.86 (s, 2H, CH_2), 4.50 (s, 6H, NH_2). ^{13}C{^{1}H} NMR (DMSO-d_6, ppm): δ 175.3, 164.4, 159.1, 145.1, 137.4, 117.5, 51.1 ppm. ^{15}N NMR (DMSO-d_6): −17.7, −30.3, −35.9, −50.2, −80.8, −151.4, −152.6, −159.3, −179.4, −192.2, −292.6, −309.0, −333.1. IR (ν, cm^{-1}): 3323, 3208, 2345, 2140, 1689, 1637, 1455, 1329, 1262, 1131, 803, 638. Elemental analysis of $C_7H_{11}N_{17}O_7$ (445.28): calcd: C 18.88, H 2.49, N 53.48%. Found: C 19.01, H 2.52, N 52.58%.

Author contributions

Priyanka Das: conceptualization, methodology, investigation, validation, formal analysis, and writing – original draft; Prachi Bhatia: methodology and writing – reviewing and editing; Krishna Pandey: methodology and writing – reviewing and editing; and Dheeraj Kumar: conceptualization, methodology, validation, formal analysis, writing – reviewing and editing, and supervision.

Conflicts of interest

There are no conflicts to declare.

Acknowledgements

The authors are grateful for the financial support from Science and Engineering Research Board (SERB/EEQ/2019/000540), New Delhi. DK acknowledges the Department of Science and Technology (DST), India, for providing financial support under the DST INSPIRE faculty award scheme [DST/INSPIRE/04/2017/001464]. We thank DST-FIST [SR/FST/CS-II/2018/72(C)] and IITR for funding the 500 MHz NMR and single-crystal X-ray diffraction facilities at IIT Roorkee. P. D. and P. B. acknowledge MHRD for research fellowships.

References

1 T. M. Klapotke, *Chemistry of High-Energy Materials*, De Gruyter, Berlin, 2019.
2 M. Gozin and L. L. Fershtat, *Nitrogen-Rich Energetic Materials*, Wiley-VCH, 2023.
3 S. Venugopalan, *Demystifying Explosives: Concepts in High Energy Materials*, Elsevier, 2015, 211–219.
4 Y. Tang, D. Kumar and J. M. Shreeve, Balancing Excellent Performance and High Thermal Stability in a Dinitropyrazole Fused 1,2,3,4-Tetrazine, *J. Am. Chem. Soc.*, 2017, **139**, 13684–13687.
5 D. Kumar and A. J. Elias, The Explosive Chemistry of Nitrogen: A Fascinating Journey From 9th Century to the Present, *Resonance*, 2019, **24**, 1253–1271.
6 D. Herweyer, J. L. Brusso and M. Murugesu, Modern trends in "Green" primary energetic materials, *New J. Chem.*, 2021, **45**, 10150–10159.
7 M. Göbel, K. Karaghiosoff, T. M. Klapötke, D. G. Piercey and J. Stierstorfer, Nitrotetrazolate-2 N-oxides and the Strategy of N-Oxide Introduction, *J. Am. Chem. Soc.*, 2010, **132**, 17216.
8 D. Kumar, G. H. Imler, D. A. Parrish and J. M. Shreeve, 3,4,5-Trinitro-1-(nitromethyl)-1*H*-pyrazole (TNNMP): a perchlorate free high energy density oxidizer with high thermal stability, *J. Mater. Chem. A*, 2017, **5**, 10437–10441.
9 G. Zhao, P. Yin, D. Kumar, G. H. Imler, D. A. Parrish and J. M. Shreeve, Bis(3-nitro-1-(trinitromethyl)1*H*-1,2,4-triazol-5-yl)methanone: an applicable and very dense green oxidizer, *J. Am. Chem. Soc.*, 2019, **141**, 19581–19584.
10 J. Zhou, J. Zhang, B. Wang, L. Qiu, R. Xu and A. B. Sheremetev, Recent synthetic efforts towards high energy density materials: How to design high-performance energetic structures?, *Firephyschem*, 2022, **2**, 83–139.
11 J. Singh, R. J. Staples and J. M. Shreeve, Increasing the limits of energy and safety in tetrazoles: dioximes as unusual precursors to very thermostable and insensitive energetic materials, *J. Mater. Chem. A*, 2023, **11**, 12896–12901.
12 (*a*) P. Bhatia, K. Pandey, B. Avasthi, P. Das, V. D. Ghule and D. Kumar, Controlling the Energetic Properties of N-Methylene-C-Linked 4-Hydroxy-3,5-dinitropyrazole- and Tetrazole-Based Compounds via a Selective Mono- and Dicationic Salt Formation Strategy, *J. Org. Chem.*, 2023, **88**, 15085–15096; (*b*) P. Bhatia, K. Pandey, P. Das and D. Kumar, Bis(dinitropyrazolyl)methanes spruced up with hydroxyl groups: high performance energetic salts with reduced sensitivity, *Chem. Commun.*, 2023, DOI: 10.1039/D3CC04445A.
13 D. Kumar, G. H. Imler, D. A. Parrish and J. M. Shreeve, A Highly Stable and Insensitive Fused Triazolo–Triazine Explosive (TTX), *Chem. – Eur. J.*, 2017, **23**, 1743–1747.
14 D. Kumar, Y. Tang, C. He, G. H. Imler, D. A. Parrish and J. M. Shreeve, Multipurpose Energetic Materials by Shuffling Nitro Groups on a 3,3′-Bipyrazole Moiety, *Chem. – Eur. J.*, 2018, **24**, 17220–17224.
15 Y. Wang, Y. Liu, Y. Liu, S. Song, Z. Yang, X. Qi, K. Wang, Q. Zhang and Y. Tian, Accelerating the discovery of insensitive high-energy-density materials by a materials genome approach, *Nat. Commun.*, 2018, **9**, 1–11.
16 K. Pandey, P. Bhatia, P. Dolui, V. D. Ghule and D. Kumar, Connecting Energetic Nitropyrazole and Nitrobenzene Moieties with C−C Bonds using Suzuki Cross-Coupling Reaction: A Novel Route to Thermally Stable Energetic Materials, *Asian J. Org. Chem.*, 2022, **11**, e202200543.
17 L. L. Fershtat, Recent advances in the synthesis and performance of 1,2,4,5-tetrazine-based energetic materials, *FirePhysChem*, 2023, **3**, 78–87.
18 P. Chen, H. Dou, J. Zhang, C. He and S. Pang, Trinitromethyl Energetic Groups Enhance High Heats of Detonation, *ACS Appl. Mater. Interfaces*, 2023, **15**, 4144–4151.
19 S. Feng, B. Zhang, C. Luo, Y. Liu, S. Zhu, R. Gou, S. Zhang, P. Yin and S. Pang, Challenging the Limitations of Tetranitro Biimidazole through Introducing a gem-Dinitromethyl Scaffold, *Org. Lett.*, 2023, **25**, 1290–1294.
20 P. Yin, J. Zhang, G. H. Imler, D. A. Parrish and J. M. Shreeve, Polynitro-Functionalized Dipyrazolo-1,3,5-triazinanes: Energetic Polycyclization toward High Density and Excellent Molecular Stability, *Angew. Chemie*, 2017, **129**, 8960–8964.
21 D. Kumar, G. H. Imler, D. A. Parrish and J. M. Shreeve, Aminoacetonitrile as precursor for nitrogen rich stable and insensitive asymmetric: N-methylene-C linked tetrazole-based energetic compounds, *J. Mater. Chem. A*, 2017, **5**, 16767–16775.
22 D. Chen, H. Yang, Z. Yi, H. Xiong, L. Zhang, S. Zhu and G. Cheng, $C_8N_{26}H_4$: An Environmentally Friendly Primary Explosive with High Heat of Formation, *Angew. Chemie*, 2018, **130**, 2103–2106.
23 M. Benz, T. M. Klapotke, J. Stierstorfer and M. Voggenreiter, Synthesis and Characterization of Binary, Highly Endothermic, and Extremely Sensitive 2,2′-Azobis(5-azidotetrazole), *J. Am. Chem. Soc.*, 2022, **144**, 6143–6147.
24 K. Pandey, P. Bhatia, K. Mohammad, V. D. Ghule and D. Kumar, Polynitro-functionalized 4-phenyl-1*H*-pyrazoles as heat-resistant explosives, *Org. Biomol. Chem.*, 2023, **21**, 6604–6616.
25 C. He, J. Zhang, D. A. Parrish and J. M. Shreeve, 4-Chloro-3,5-dinitropyrazole: A precursor for promising insensitive energetic compounds, *J. Mater. Chem. A*, 2013, **1**, 2863–2868.
26 X. Y. Zhang, X. Y. Lin, B. Y. Guo, C. Tan and Y. Han, Efficient synthesis of the promising energetic material precursor 4-azido-3,5-dinitro-1*H*-pyrazole with high detonation performance, *J. Mol. Struct.*, 2022, **1267**, 133526.
27 D. Kumar, G. H. Imler, D. A. Parrish and J. M. Shreeve, N-Acetonitrile Functionalized Nitropyrazoles: Precursors to

Insensitive Asymmetric N-Methylene-C Linked Azoles, *Chem. – Eur. J.*, 2017, **23**, 7876–7881.
28 P. Yin, J. Zhang, D. A. Parrish and J. M. Shreeve, Energetic N,N′-Ethylene-Bridged Bis(nitropyrazoles): Diversified Functionalities and Properties, *Chem. – Eur. J.*, 2014, **20**, 16529–16536.
29 D. Kumar, C. He, L. A. Mitchell, D. A. Parrish and J. M. Shreeve, Connecting energetic nitropyrazole and aminotetrazole moieties with: N,N′-ethylene bridges: a promising approach for fine tuning energetic properties, *J. Mater. Chem. A*, 2016, **4**, 9220–9228.
30 D. Kumar, G. H. Imler, D. A. Parrish and J. M. Shreeve, Resolving synthetic challenges faced in the syntheses of asymmetric: N,N′-ethylene-bridged energetic compounds, *New J. Chem.*, 2017, **41**, 4040–4047.
31 D. Kumar, L. A. Mitchell, D. A. Parrish and J. M. Shreeve, Asymmetric: N,N′-ethylene-bridged azole-based compounds: Two way control of the energetic properties of compounds, *J. Mater. Chem. A*, 2016, **4**, 9931–9940.
32 W. L. Cao, Q. U. N. Tariq, Z. M. Li, J. Q. Yang and J. G. Zhang, Recent advances on the nitrogen-rich 1,2,4-oxadiazole-azoles-based energetic materials, *Def. Technol.*, 2022, **18**, 344–367.
33 F. Yang, P. Zhang, X. Zhou, Q. Lin, P. Wang and M. Lu, Combination of Polynitropyrazole and 5-Amino-1,2,4-oxadiazole Derivatives: An Approach to High Performance Energetic Materials, *Cryst. Growth Des.*, 2020, **20**, 3737–3746.
34 Q. Wang, Y. Shao and M. Lu, $C_8N_{12}O_8$: a promising insensitive high-energy-density material, *Cryst. Growth Des.*, 2018, **18**, 6150–6154.
35 Z. Fu, R. Su, Y. Wang, Y. F. Wang, W. Zeng, N. Xiao, Y. Wu, Z. Zhou, J. Chen and F. X. Chen, Synthesis and characterization of energetic 3-nitro-1,2,4-oxadiazoles, *Chem. – Eur. J.*, 2012, **18**, 1886–1889.
36 Y. Liu, C. He, J. M. Shreeve, G. H. Imler and D. A. Parrish, Asymmetric nitrogen-rich energetic materials resulting from the combination of tetrazolyl, dinitromethyl and (1,2,4-oxadiazol-5-yl)nitroamino groups with furoxan, *Dalton Trans.*, 2018, **47**, 16558–16566.
37 Y. Zhang, Y. Guo, Y. H. Joo, D. A. Parrish and J. M. Shreeve, 3,4,5-Trinitropyrazole-based energetic salts, *Chem. – Eur. J.*, 2010, **16**, 10778–10784.
38 M. Wolff, D. J. Grimwood, J. J. McKinnon, M. J. Turner, D. Jayatilaka and M. A. Spackman, *Crystal Explorer 17.5*, 2012.
39 E. R. Johnson, S. Keinan, P. Mori-Sánchez, J. Contreras-García, A. J. Cohen and W. Yang, Revealing Noncovalent Interactions, *J. Am. Chem. Soc.*, 2010, **132**, 6498–6506.
40 T. Lu and F. Chen, Multiwfn: A multifunctional wavefunction analyzer, *J. Comput. Chem.*, 2012, **33**, 580–592.
41 W. Humphrey, A. Dalke and K. Schulten, Sartorius Products, *J. Mol. Graphics*, 1996, **14**(October 1995), 33–38.
42 *SMART: Bruker Molecular Analysis Research Tools, version 5.618, Bruker Analytical X-ray Systems*, Madison, WI, 2000.
43 R. G. Parr and W. Yang, *Density Functional Theory of Atoms and Molecules*, Oxford University Press, New York, 1989.
44 M. J. Frisch, G. W. Trucks, H. B. Schlegel, G. E. Scuseria, M. A. Robb, J. R. Cheeseman, G. Scalmani, V. Barone, G. A. Petersson, H. Nakatsuji, X. Li, M. Caricato, A. Marenich, J. Bloino, B. G. Janesko, R. Gomperts, B. Mennucci, H. P. Hratchian, J. V. Ortiz, A. F. Izmaylov, J. L. Sonnenberg, D. Williams-Young, F. Ding, F. Lipparini, F. Egidi, J. Goings, B. Peng, A. Petrone, T. Henderson, D. Ranasinghe, V. G. Zakrzewski, J. Gao, N. Rega, G. Zheng, W. Liang, M. Hada, M. Ehara, K. Toyota, R. Fukuda, J. Hasegawa, M. Ishida, T. Nakajima, Y. Honda, O. Kitao, H. Nakai, T. Vreven, K. Throssell, J. A. Montgomery Jr, J. E. Peralta, F. Ogliaro, M. Bearpark, J. J. Heyd, E. Brothers, K. N. Kudin, V. N. Staroverov, T. Keith, R. Kobayashi, J. Normand, K. Raghavachari, A. Rendell, J. C. Burant, S. S. Iyengar, J. Tomasi, M. Cossi, J. M. Millam, M. Klene, C. Adamo, R. Cammi, J. W. Ochterski, R. L. Martin, K. Morokuma, O. Farkas, J. B. Foresman and D. J. Fox, *Gaussian 09, Revision E.01*, Gaussian, Inc., Wallingford, CT, 2013.
45 E. F. C. Byrd and B. M. Rice, Improved prediction of heats of formation of energetic materials using quantum mechanical calculations, *J. Phys. Chem. A*, 2006, **110**, 1005–1013.
46 H. D. B. Jenkins, D. Tudela and L. Glasser, Lattice potential energy estimation for complex ionic salts from density measurements, *Inorg. Chem.*, 2002, **41**, 2364–2367.
47 V. D. Ghule, Computational screening of nitrogen-rich energetic salts based on substituted triazine, *J. Phys. Chem. C*, 2013, **117**, 16840–16849.